LTH 1092, CERN-TH-2016-161

Indirect probes of the trilinear Higgs coupling: $gg \to h$ and $h \to \gamma\gamma$

Martin Gorbahn[1] **and Ulrich Haisch**[2,3]

[1] *Department of Mathematical Sciences, University of Liverpool, L69 7ZL Liverpool, United Kingdom*

[2] *Rudolf Peierls Centre for Theoretical Physics, University of Oxford, OX1 3NP Oxford, United Kingdom*

[3] *CERN, Theory Division, CH-1211 Geneva 23, Switzerland*

E-mail: Martin.Gorbahn@liverpool.ac.uk, ulrich.haisch@physics.ox.ac.uk

In the framework of the Standard Model effective field theory, we examine the indirect constraints on the trilinear Higgs coupling λ that arise from Higgs production in gluon-gluon-fusion and diphoton Higgs decays. We calculate 2-loop contributions to the $gg \to h$ and $h \to \gamma\gamma$ amplitudes that are affected by modifications of the trilinear Higgs-boson vertex. Based on our new results, we analyse the sensitivity of present and future measurements of the hgg and $h\gamma\gamma$ couplings to shifts in λ. Under the assumption that $O_6 = -\lambda \left(H^\dagger H\right)^3$ is the only dimension-6 operator that alters the trilinear Higgs interactions, we find that at present the considered loop-level probes provide stronger constraints than $pp \to 2h$. At future high-energy colliders indirect $\mathcal{O}(5)$ determinations of the trilinear Higgs coupling may be possible, making precision measurements of $gg \to h$ and $h \to \gamma\gamma$ a useful addition to direct extractions of λ through double-Higgs production.

Contents

1 Introduction 1

2 Preliminaries 3

3 Anomalous dimensions 4

4 Finite corrections to $gg \to h$ and $h \to \gamma\gamma$ 5

5 Constraints from double-Higgs production 8

6 Constraints from Higgs production and diphoton decay 9

7 Conclusions 11

A Non-physical operators 12

B Feynman rules 12

C Renormalisation procedure for $gg \to h$ and $h \to \gamma\gamma$ 13

D Unphysical Higgs sector 14

1 Introduction

The discovery of a boson and measurements of its production and decay rates at the Large Hadron Collider (LHC) give convincing evidence for the Higgs mechanism in which a linearly realised $SU(2)_L \times U(1)_Y$ symmetry is spontaneously broken to $U(1)_{\rm EM}$ by the vacuum expectation value (VEV) of the Higgs field. The new state seems to behave like a CP-even scalar and has couplings to the gauge bosons and fermions that agree with those predicted by the Standard Model (SM) at the level of 20% to 100% [1, 2]. The strength of the Higgs couplings to the other SM fields will be further scrutinised at forthcoming LHC runs and (possibly) other future high-energy colliders such as an International Linear Collider or a Future Circular Collider (FCC).

The mechanism of electroweak symmetry breaking (EWSB) is in contrast to the Higgs gauge boson and fermion couplings essentially unexplored. Within the SM, the mass and the self-interactions of the physical Higgs field h are parametrised by the potential

$$V_{\rm SM} = \frac{m_h^2}{2}\, h^2 + \lambda v\, h^3 + \frac{\kappa}{4}\, h^4 \,, \tag{1.1}$$

where $v \simeq 246\,\text{GeV}$ denotes the Higgs VEV and

$$\lambda = \kappa = \frac{m_h^2}{2v^2}\,. \tag{1.2}$$

The LHC measurement of the Higgs-boson mass leading to $m_h \simeq 125\,\text{GeV}$, probes the first term in (1.1), but the h^3 and h^4 couplings, and in particular the SM relation (1.2) have not been tested. Determinations of the Higgs self-couplings are therefore an essential task that might provide indirect access to beyond the SM (BSM) dynamics, or if no significant deviations from (1.2) are found, will further add to the impressive track record of the SM.

High-energy collider allow to probe the coefficients λ and κ in (1.1) through double-Higgs and triple-Higgs production, respectively. At 14 TeV centre-of-mass energy, the cross section for $pp \to 3h$ production is of $\mathcal{O}(0.1\,\text{fb})$, which even at the high-luminosity LHC (HL-LHC) renders any meaningful extraction of κ impossible (see for instance [3–5]). The prospect to observe double-Higgs production at the HL-LHC is significantly better since at 14 TeV the $pp \to 2h$ production cross section amounts to $\mathcal{O}(35\,\text{fb})$ [6–12]. LHC detections of double-Higgs production still remain challenging (cf. [13–29]) and in consequence even with the full HL-LHC data set of $3\,\text{ab}^{-1}$ only an $\mathcal{O}(1)$ determination of the trilinear Higgs coupling seems feasible under optimistic assumptions.

This raises the question if it is possible to constrain λ by other (possibly complementary) means. As pointed out in [30], one way to achieve sensitivity to the h^3 coupling is provided through precision studies of the process $e^+e^- \to hZ$, which receives 1-loop corrections proportional to λ from Feynman diagrams with virtual Higgses and/or a Z boson (see more recently also [31]). While loop-level probes of the h^3 vertex can clearly not replace extractions of λ based on collider measurements of double-Higgs production, they might be crucial in resolving degeneracies in parameter space. This is evident by recalling that $gg \to 2h$ production is itself a quantum process that depends not only on the strength of the h^3 interaction, but also on the top-quark Yukawa coupling as well as all the masses and all the Higgs couplings of the possible BSM particles circulating in the loop graphs.

The main purpose of our work is to illustrate other ways to indirectly probe the coefficient λ entering (1.1). To keep our discussion as model-independent as possible, we will use an effective field theory (EFT) in which the SM Lagrangian is the leading term and BSM effects are encoded in dimension-6 operators constructed solely out of SM fields. In this framework, we calculate 2-loop contributions to the $gg \to h$ and $h \to \gamma\gamma$ amplitudes that are affected by modifications of the h^3 vertex. This calculation involves both the computation of the relevant anomalous dimensions of the operators as well as the computation of finite corrections at the weak scale. Based on our results, we analyse the sensitivity of present and future measurements of the hgg and the $h\gamma\gamma$ couplings to shifts in the trilinear Higgs interactions. We find that our new loop-level probes provide interesting and meaningful model-independent constraints on λ, in the simplified case that the operator $O_6 = -\lambda\left(H^\dagger H\right)^3$ furnishes the sole modification of the h^3 vertex. Applying our findings to ultraviolet (UV) complete realisations of BSM physics is left for further study.

This article is structured as follows. In Section 2 we introduce the effective interactions relevant for our paper. The results of our 2-loop calculations are presented in Sections 3

and 4. Our numerical analyses are performed in Sections 5 and 6. We conclude in Section 7. Some technical details of our computations are described in Appendix A, B, C and D.

2 Preliminaries

New physics can be described in a model-independent way by augmenting the SM Lagrangian $\mathcal{L}_{\rm SM}$ by $SU(3)_C \times SU(2)_L \times U(1)_Y$ gauge-invariant higher-dimensional operators. In our work, we consider the effective Lagrangian

$$\mathcal{L}^{(6)} = \sum_k \frac{\bar{c}_k}{v^2}\, O_k \,, \tag{2.1}$$

built out of the following dimension-6 operators

$$\begin{aligned}
O_6 &= -\lambda \left(H^\dagger H\right)^3 , \\
O_H &= \frac{1}{2}\, \partial_\mu \big(H^\dagger H\big)\, \partial^\mu \big(H^\dagger H\big) , \\
O_T &= \frac{1}{2}\, \big(H^\dagger \overleftrightarrow{D}_\mu H\big)\big(H^\dagger \overleftrightarrow{D}^\mu H\big) , \\
O_W &= \frac{4i}{g}\, \big(H^\dagger \tau^i \overleftrightarrow{D}_\mu H\big) D_\nu W^{i,\mu\nu} , \\
O_B &= \frac{2ig'}{g^2}\, \big(H^\dagger \overleftrightarrow{D}_\mu H\big) D_\nu B^{\mu\nu} , \\
O_{HW} &= \frac{8i}{g}\, \big(D_\mu H^\dagger \tau^i D_\nu H\big) W^{i,\mu\nu} , \\
O_{HB} &= \frac{4ig'}{g^2}\, \big(D_\mu H^\dagger D_\nu H\big) B^{\mu\nu} , \\
O_{GG} &= \frac{2g_s}{g^2}\, H^\dagger H\, G^a_{\mu\nu} G^{a,\mu\nu} , \\
O_{BB} &= \frac{2g'}{g^2}\, H^\dagger H\, B_{\mu\nu} B^{\mu\nu} , \\
O_u &= -Y_u\, H^\dagger H\, \bar{Q}_L u_R \tilde{H} , \\
O_d &= -Y_d\, H^\dagger H\, \bar{Q}_L d_R H , \\
O_\ell &= -Y_\ell\, H^\dagger H\, \bar{L}_L \ell_R H .
\end{aligned} \tag{2.2}$$

Here λ denotes the SM Higgs self-coupling introduced in (1.2), H is the SM Higgs doublet and we have used the shorthand notation $\tilde{H}^i = \epsilon_{ij} \left(H^j\right)^*$ with ϵ_{ij} totally antisymmetric and $\epsilon_{12} = 1$. The covariant derivative operator $\overleftrightarrow{D}_\mu$ is defined as $H^\dagger \overleftrightarrow{D}_\mu H = H^\dagger D_\mu H - \big(D_\mu H^\dagger\big) H$ and $\tau^i = \sigma^i/2$ with σ^i the usual Pauli matrices. The coupling constants of the gauge groups $SU(3)_C$, $SU(2)_L$ and $U(1)_Y$ are denoted by g_s, g and g', while $G^a_{\mu\nu}$, $W^i_{\mu\nu}$, and $B_{\mu\nu}$ are the corresponding field strength tensors. The Yukawa couplings Y_u, Y_d and Y_ℓ are matrices in flavour space and a sum over flavours indices is implicit in (2.2). Finally,

Q_L, L_L denote left-handed quark and lepton doublets, while u_R, d_R, ℓ_R are right-handed fermion singlets.

After EWSB, the $SU(3)_C \times SU(2)_L \times U(1)_Y$ gauge-invariant operators introduced in (2.2) modify the couplings of the Higgs boson to itself, to vector bosons and fermions. We write the couplings that result from $\mathcal{L}_{\rm SM} + \mathcal{L}^{(6)}$ and that are relevant for our article as follows

$$\mathcal{L} \supset -\lambda c_3 v h^3 + c_g \frac{h}{v} G^a_{\mu\nu} G^{a,\mu\nu} + c_\gamma \frac{h}{v} F_{\mu\nu} F^{\mu\nu} \,, \tag{2.3}$$

where $F_{\mu\nu} = \partial_\mu A_\nu - \partial_\mu A_\nu$ with A_μ the photon field. Upon canonical normalisation of the Higgs kinetic term the tree-level coefficient c_3 takes the form

$$c_3 = 1 + \bar{c}_6 - \frac{3\bar{c}_H}{2} \,. \tag{2.4}$$

The coefficients c_g and c_γ arise first at the 1-loop level and we will give the relevant expressions below. Note that the Wilson coefficients c_k as well as the trilinear Higgs coupling λ appearing in (2.3) are all understood to be evaluated at the weak scale, which we will denote by μ_w hereafter.

A final comment concerns the impact of operators with dimension larger than six. Including for instance a dimension-8 term of the form

$$\mathcal{L}^{(8)} \supset -\frac{\lambda \bar{c}_8}{v^4} \left(H^\dagger H\right)^4 \,, \tag{2.5}$$

would also result in a modification of the trilinear Higgs coupling and the coefficient c_3 introduced in (2.3) would receive an additional additive contribution of $2\bar{c}_8$ in (2.4). In a given weakly-coupled UV-complete theory the Wilson coefficients $\bar{c}_6$, c_H and $\bar{c}_8$ could be calculated by integrating out heavy degrees of freedom and matching onto $\mathcal{L}^{(6)} + \mathcal{L}^{(8)}$. The important point is however that the indirect probes of the Higgs trilinear coupling proposed in our work measure c_3, i.e. the coefficient multiplying the interaction term $-\lambda v h^3$, so that one does not need to know the precise form of the latter coefficient. In the following we will focus our attention on BSM scenarios where the Wilson coefficient $\bar{c}_6$ furnishes the sole modification of the h^3 vertex and in consequence formulate the results presented in Sections 4 to 6 in terms of $\bar{c}_6$. The dependence on c_3 could however be easily restored by replacing $\bar{c}_6$ with $c_3 - 1$ in all relevant formulas.

3 Anomalous dimensions

The primary goal of this article is to determine the dominant corrections to the Higgs couplings to gluon and photon pairs (2.3) that result from the effective operator O_6. In fact, there are two different kinds of such contributions. First, corrections enhanced by logarithms $\ln\left(\Lambda^2/\mu_w^2\right)$ which arise from the renormalisation group (RG) evolution

$$\frac{d\bar{c}_k}{d\ln\mu} = \gamma_{k6}\, \bar{c}_6 \,, \tag{3.1}$$

of the Wilson coefficients $\bar{c}_k$ from the new-physics scale Λ down to μ_w, if the operator O_6 mixes into O_k. Second, finite corrections that stem from the calculation of $gg \to h$

and $h \to \gamma\gamma$ Green's functions with modified h^3 vertices. In the following, we discuss the logarithmically-enhanced corrections associated to the RG evolution, turning our attention to the finite contributions in the next section.

Since a non-zero initial condition $\bar{c}_6$ at Λ does not affect the other weak-scale Wilson coefficients $\bar{c}_k$ at the 1-loop level [32–35], the leading logarithmic corrections to (2.3) proportional to $\bar{c}_6$ have to arise from 2-loop diagrams. In order to determine the mixing of O_6 into the set of operators introduced in (2.2) we have calculated the 2-loop matrix elements $HH \to HH$, $HH \to BB$, $HH \to WW$, $HH \to BW$ and $HHH \to f\bar{f}$ involving a single insertion of O_6. The pole parts of the graphs have been evaluated using the method described for instance in [36–38]. Specifically, we have performed the calculation off-shell in an arbitrary R_ξ gauge which allows us to explicitly check the ξ-independence of the mixing among physical operators. To distinguish between infrared (IR) and UV divergences, a common mass M for all fields is introduced, expanding the loop integrals in inverse powers of M. This makes the calculation of the 2-loop UV divergences straightforward, because after Taylor expansion in the external momenta, M becomes the only relevant internal scale and 2-loop tadpole integrals with a single non-zero mass are known [39]. Further technical details on our off-shell calculation are given in Appendix A.

We find that the only non-vanishing anomalous dimensions γ_{k6} that encode the 2-loop off-diagonal mixing of O_6 into the operators of (2.2) are

$$\gamma_{H6} = \frac{1}{16\pi^4}\, 12\lambda^2\,, \qquad \gamma_{f6} = -\frac{1}{16\pi^4}\left(\lambda^2 + 3\,Y_f Y_f^\dagger\right)\,, \tag{3.2}$$

where $f = u, d, \ell$. These results imply that the weak-scale Wilson coefficients of O_H and O_f alone receive logarithmically-enhanced contributions $\ln\left(\Lambda^2/\mu_w^2\right)$ proportional to $\bar{c}_6$ at the 2-loop level. In this context it is also important to realise that the higher-dimensional interactions introduced in (2.2) provide just a subset of the dimension-6 operators of the full SM effective Lagrangian (cf. [40, 41]). In particular, operators that are composed out of three field strength tensors such as $O_{3W} = 4g^2\,\epsilon_{ijk} W^i_{\mu\nu} W^{j,\nu}_\rho W^{k,\rho\mu}$ with ϵ_{ijk} the Levi-Civita tensor are not included in $\mathcal{L}^{(6)}$. Since O_6 involves three powers of $H^\dagger H$ it however cannot give rise to amplitudes like $W \to WW$ at two loops, because one has to contract all H fields to obtain a non-zero matrix element. Since this is first possible at the 3-loop level, all 2-loop anomalous dimensions describing the mixing of O_6 into dimension-6 operators containing only field strength tensors vanish identically. Beyond that order such mixings are likely to be present, but a computation of these logarithmic 3-loop corrections is beyond the scope of this work.

4 Finite corrections to $gg \to h$ and $h \to \gamma\gamma$

As already mentioned, a second type of contributions to the coefficients c_g and c_γ entering (2.3) originate from the calculation of $gg \to h$ and $h \to \gamma\gamma$ Green's functions involving interaction vertices that are modified by the presence of O_6.

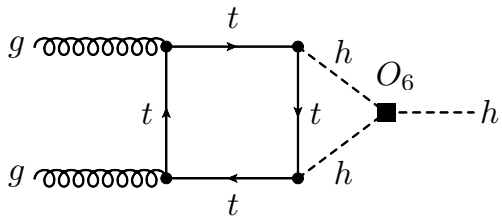

Figure 1. Example of a 2-loop diagram with an insertion of the effective operator O_6 that contributes to the $gg \to h$ amplitude at $\mathcal{O}(\lambda)$.

We first discuss the corrections arising in the case of the $gg \to h$ amplitude. Expanding the corresponding Wilson coefficient c_g as follows

$$c_g = \frac{\alpha_s}{\pi} \left(c_g^{(0)} + \frac{\lambda}{(4\pi)^2} c_g^{(1)} \right) , \tag{4.1}$$

one obtains at the 1-loop level

$$c_g^{(0)} = \sum_q A_q \simeq 0.081 + 0.007\, i \,, \tag{4.2}$$

where the sum runs over all quarks and

$$A_f = \frac{\tau_f}{8} \left[1 + (1 - \tau_f) \arctan^2 \frac{1}{\sqrt{\tau_f - 1}} \right] , \tag{4.3}$$

with $\tau_f = 4m_f^2/m_h^2$. The numerical value given in (4.2) corresponds to $m_t \simeq 163.3\,\text{GeV}$, $m_b \simeq 4.2\,\text{GeV}$, $m_c \simeq 1.3\,\text{GeV}$ and $m_h \simeq 125\,\text{GeV}$. Since the on-shell 1-loop form factor A_f approaches $1/12$ for $\tau_f \to \infty$ and vanishes proportional to τ_f in the limit $\tau_f \to 0$, it is an excellent approximation to include only the top quark in the sum appearing in (4.2) and to take the infinite quark-mass limit. In such a case, one arrives at the classic Shifman-Vainshtein-Zakharov result $c_g^{(0)} = 1/12 \simeq 0.083$ derived first in [42].

The $\mathcal{O}(\lambda)$ correction to the coefficient c_g arises from both 2-loop Feynman diagrams and 1-loop counterterm graphs involving a Higgs wave function renormalisation. To find the former type of contribution, we apply EFT techniques (see for instance [43] for a non-trivial application to Higgs production) and employ a hard-mass expansion procedure $\tau_t \to \infty$ to the full 2-loop diagrams involving a top-quark loop and a h^3 vertex that arises from the insertion of O_6. A prototype graph of such a contribution is shown in Figure 1. After setting $m_h = 0$ and Taylor expanding in the external momenta, this technique reduces the calculation to the evaluation of 2-loop vacuum bubbles with a single mass scale, which can all be expressed in terms of Gamma functions (cf. [39]).

The correction proportional to the $\mathcal{O}(\lambda)$ contribution to the Higgs wave function renormalisation constant

$$Z_h = 1 + \frac{\lambda}{(4\pi)^2} Z_h^{(1)} , \tag{4.4}$$

is instead found from the 1-loop Higgs-boson selfenergy with one and two insertions of O_6. By a straightforward calculation, we obtain the analytic result

$$Z_h^{(1)} = \left(9 - 2\sqrt{3}\pi\right) \bar{c}_6 \left(\bar{c}_6 + 2\right) . \tag{4.5}$$

Combining both contributions, we arrive at

$$c_g^{(1)} = -\frac{1}{12}\left(\frac{1}{4} + 3\ln\frac{\mu_w^2}{m_t^2}\right)\bar{c}_6 + \frac{Z_h^{(1)}}{2}\, c_g^{(0)} , \tag{4.6}$$

with $c_g^{(0)}$ given in (4.2). As a powerful cross-check of our calculation, we have extracted the $\mathcal{O}(\lambda)$ correction to the coefficient c_g also from the 2-loop $gg \to 2h$ and $gg \to 3h$ Green's functions, obtaining in all three cases the exact same result. Details on the renormalisation of the bare 2-loop $gg \to h$ amplitude can be found in Appendix C. Notice that the first term in (4.6) represents only the leading term in the asymptotic expansion of the $\mathcal{O}(\lambda)$ correction to the on-shell $gg \to h$ form factor. To determine whether our analytic expression for $c_g^{(1)}$ approximates the full result well would require an explicit calculation of the relevant $gg \to h$ amplitudes that does not rely on the heavy-quark expansion for what concerns the 2-loop contributions. Such a computation is however beyond the scope of our article.

In the case of the $h \to \gamma\gamma$ transition, we write

$$c_\gamma = \frac{\alpha}{\pi}\left(c_\gamma^{(0)} + \frac{\lambda}{(4\pi)^2}\, c_\gamma^{(1)}\right) , \tag{4.7}$$

where the 1-loop contribution is given by

$$c_\gamma^{(0)} = A_W + \sum_f 2N_C^f Q_f^2 A_f \simeq -0.82 - 0.01\, i\, . \tag{4.8}$$

Here $N_C^q = 3$ and $N_C^\ell = 1$ are colour factors, the sum runs over all electrically charged fermions carrying charge $Q_u = 2/3$, $Q_d = -1/3$ and $Q_\ell = -1$, A_f has been introduced in (4.3) and

$$A_W = -\frac{1}{8}\left[2 + 3\tau_W + 3\tau_W(2-\tau_W)\arctan^2\frac{1}{\sqrt{\tau_W - 1}}\right] , \tag{4.9}$$

with $\tau_W = 4m_W^2/m_h^2$. In order to obtain the numerical result in (4.8), we have employed $m_W \simeq 80.4\,\text{GeV}$ and $m_\tau \simeq 1.777\,\text{GeV}$. Numerically, one has furthermore $A_W \simeq -1.04$, while in the limit $\tau_W \to \infty$ ($\tau_W \to 0$) the on-shell 1-loop form factor A_W tends to the constant value $-7/8$ ($-1/4$). In the infinite mass limit $\tau_{t,W} \to \infty$, one therefore finds that $c_\gamma^{(0)} = -47/72 \simeq -0.65$. Notice that compared to the case of A_f the heavy-mass expansion works less well for A_W, but still captures around 85% of the exact 1-loop result. Motivated by this observation we again apply a hard-mass expansion procedure to obtain an approximation for the 2-loop corrections to c_γ involving $W^\pm$ ($\phi^\pm$) exchanges.

Since after EWSB the operator O_6 modifies both the trilinear Higgs coupling as well as the coupling between two Higgses and two charged would-be Goldstone bosons (see (B.2)), one naively has to consider 2-loop diagrams that contain both a h^3 and a $h^2\phi^+\phi^-$ vertex. A possible graph of each type is depicted in Figure 2. To maintain gauge invariance at the

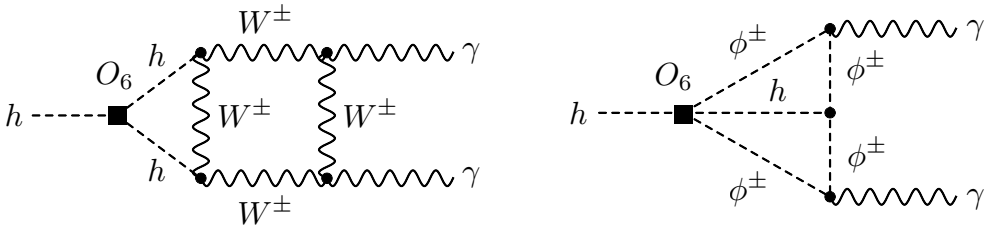

Figure 2. Left: Example of a 2-loop diagram involving a h^3 vertex that in the limit $m_W \gg m_h$ gives rise to $h \to \gamma\gamma$ at $\mathcal{O}(\lambda)$. Right: A possible 2-loop graph with a $h\phi^+\phi^-$ vertex. For $m_h = 0$, diagrams of this type do however not contribute to $h \to \gamma\gamma$ at $\mathcal{O}(\lambda)$. For additional explanations see text.

level of off-shell Green's functions, we use the 't Hooft-Feynman version of the background field gauge for the external photon fields (see e.g. [44]) when calculating these diagrams. In this gauge there is no $\gamma W^\pm \phi^\mp$ vertex and as a result all 2-loop graphs involving a $h^2\phi^+\phi^-$ interaction necessarily also contain a $h\phi^+\phi^-$ vertex. Since the Feynman rule of the $h\phi^+\phi^-$ coupling is proportional to m_h^2/m_W, it then follows that diagrams with a $h^2\phi^+\phi^-$ vertex do not contribute to $c_\gamma^{(1)}$ in the limit $\tau_W \to \infty$. We have verified this feature by an explicit calculation of the corresponding 2-loop graphs.

Combining the 2-loop gauge boson and top-quark contributions and including the correction due to the wave function renormalisation of the Higgs boson, we find for $\tau_{t,W} \to \infty$ the following analytic expression

$$c_\gamma^{(1)} = -\frac{7}{8}\left(\frac{9}{7} - \frac{22}{7}\ln\frac{\mu_w^2}{m_W^2}\right)\bar{c}_6 - \frac{2}{9}\left(\frac{1}{4} + 3\ln\frac{\mu_w^2}{m_t^2}\right)\bar{c}_6 + \frac{Z_h^{(1)}}{2}\,c_\gamma^{(0)}\,, \tag{4.10}$$

with $Z_h^{(1)}$ and $c_\gamma^{(0)}$ given in (4.5) and (4.8), respectively. The necessary ingredients to obtain the above result are presented in Appendix C, while the renormalisation of the would-be Goldstone boson sector is discussed in Appendix D.

5 Constraints from double-Higgs production

In the next section will derive existing and possible future limits on the modifications of the h^3 coupling that arise from $gg \to h$ and $h \to \gamma\gamma$. All the numbers that we will present below should be compared to the bounds on the trilinear Higgs coupling that one can obtain by studying double-Higgs production at the LHC.

In fact, ATLAS has combined the full 8 TeV data set corresponding to $20.3\,\text{fb}^{-1}$ of integrated luminosity to search for $2h \to 2b2\tau, 2\gamma 2W, 2\gamma 2b$ and $4b$ [45–47]. While no evidence for double-Higgs production is observed, a 95% confidence level (CL) upper limit of 0.69 pb is set on the production cross section, which is about 70 times above the SM expectation of (9.9 ± 1.3) fb [10]. To derive a bound on $\bar{c}_6$, we use the `MadGraph5_aMC@NLO` [48] implementation of cross section computations for loop-induced processes [49] as well as `HPAIR` [50, 51].

For pp collisions at 8 TeV, we obtain

$$\sigma(pp \to 2h) = (9.9 \pm 1.3)\left(1 - 0.87\bar{c}_6 + 0.33\bar{c}_6^2\right)\text{fb}\,, \tag{5.1}$$

if only the Wilson coefficient $\bar{c}_6$ is allowed to be non-zero, but the remaining coefficients $\bar{c}_k$ of the operators entering (2.2) are assumed to vanish. Taking into account theoretical uncertainties, we find from this formula that the ATLAS limit on the $pp \to 2h$ production cross section translates into the following 95% CL bound

$$\bar{c}_6 \in [-15.5, 18.1]\,. \tag{5.2}$$

This limit implies that the combination $\lambda\bar{c}_3$ introduced in (2.3) can at present still deviate from the SM trilinear Higgs coupling λ by a factor of about 17. This finding agrees with the conclusion drawn in [28].

At the HL-LHC with $3\,\text{ab}^{-1}$ of integrated luminosity the constraints on the trilinear Higgs coupling are expected to improve considerably (cf. [13–29]). For example, the ATLAS study [26] implies that the ultimate sensitivity that the LHC can reach in the $2h \to 2b2\gamma$ channel, will allow to set a 95% CL bound of

$$\bar{c}_6 \in [-2.3, 7.7]\,, \tag{5.3}$$

on the coefficient of the dimension-6 operator O_6. In order to allow for a better comparison with (5.2) and the bounds derived in the next section, the quoted limit again assumes that $\bar{c}_6$ is the only numerically relevant Wilson coefficient at the weak scale. If this assumption is relaxed the limit (5.3) can worsen by a factor of a few [25, 27]. Notice finally that (5.3) exhibits two solutions. The first one is located close to the SM point at $\bar{c}_6 = 0$, while the second solution at $\bar{c}_6 \simeq 5.7$ corresponds to the case where the $gg \to 2h$ amplitude has an opposite sign with respect to the SM. Removing the non-SM solution seems challenging at the HL-LHC, but should be possible at a 100 TeV FCC-pp [27].

6 Constraints from Higgs production and diphoton decay

In the following, we study the present constraints and the future sensitivities on the trilinear Higgs coupling that are provided by $gg \to h$ and $h \to \gamma\gamma$. In order to allow for an easy comparison with the results (5.2) and (5.3), we will throughout assume that the modifications of the Wilson coefficient of the operator O_6 furnish the dominant contribution to the observable under consideration, and consequently neglect effects associated to the remaining $\bar{c}_k$ in (2.1).

The ratio of the cross sections for Higgs-boson production in gluon-gluon fusion and the modification of the signal strength for Higgs decays into two photons can be written as

$$\mu_{gg} = \frac{\sigma(gg \to h)}{\sigma_{\text{SM}}(gg \to h)} = |\kappa_g|^2\,, \qquad \mu_{\gamma\gamma} = \frac{\Gamma(h \to \gamma\gamma)}{\Gamma_{\text{SM}}(h \to \gamma\gamma)} = |\kappa_\gamma|^2\,, \tag{6.1}$$

respectively. From the definitions (4.1) and (4.7) it is then readily seen that ($i = g, \gamma$)

$$\kappa_i \simeq 1 + \frac{\lambda}{(4\pi)^2}\frac{\text{Re}\,c_i^{(1)}}{\text{Re}\,c_i^{(0)}}\,, \tag{6.2}$$

where we have neglected the small imaginary parts of $c_i^{(0)}$ and $c_i^{(1)}$.

In order to set limits on the Wilson coefficient $\bar{c}_6$, we use the latest results of a global fit to the Higgs production channels performed by ATLAS [1] and CMS [2], where the effective couplings κ_g, κ_γ and $\kappa_{\gamma Z}$ are left to vary freely. All the remaining couplings are set to their SM values. ATLAS and CMS obtain $\kappa_g = 1.12 \pm 0.12$, $\kappa_\gamma = 1.00 \pm 0.12$ and $\kappa_g = 0.89 \pm 0.10$, $\kappa_\gamma = 1.15 \pm 0.13$, respectively. Performing a naive weighted average, one finds

$$\kappa_g = 0.98 \pm 0.08\,, \qquad \kappa_\gamma = 1.07 \pm 0.09\,. \tag{6.3}$$

Employing now (4.2), (4.6), (4.8), (4.10), identifying $\mu_w = m_h \simeq 125\,\text{GeV}$ and treating the extractions of κ_g and κ_γ as uncorrelated, these limits translate into

$$\bar{c}_6 \in [-12.7, 9.9]\,, \tag{6.4}$$

at 95% CL. One observes that the present indirect constraint arising from a combination of the observed $gg \to h$ and $h \to \gamma\gamma$ signal strengths is more restrictive than the direct bound (5.2) from $pp \to 2h$ production. We believe that this is an interesting finding, because it shows that it is possible to constrain the h^3 couplings at a pp collider by means other than double-Higgs production.

Since at the time the LHC has collected $3\,\text{ab}^{-1}$ of data, the effective hgg and $h\gamma\gamma$ couplings will be known much more accurately than today as well, it is also interesting to study the prospects of the indirect probes provided by $gg \to h$ and $h \to \gamma\gamma$. The sensitivity study [52] finds for instance that compared to (6.3) the precision on κ_g (κ_γ) might be improved by a factor of 3 (4). Assuming that the central values of the future LHC measurements end up being spot on the SM, this means

$$\kappa_g = 1.00 \pm 0.03\,, \qquad \kappa_\gamma = 1.00 \pm 0.02\,. \tag{6.5}$$

The corresponding 95% CL limit on the Wilson coefficient of O_6 reads

$$\bar{c}_6 \in [-8.0, 5.1]\,. \tag{6.6}$$

With such a precision one will start to become sensitive to the flipped-sign solution in (5.3).

At a e^+e^- option of a FCC (FCC-ee), the bounds (6.5) may even be further tightened [53], possibly leading to

$$\kappa_g = 1.00 \pm 0.01\,, \qquad \kappa_\gamma = 1.00 \pm 0.015\,. \tag{6.7}$$

With this sensitivity, one could set the following 95% CL limit

$$\bar{c}_6 \in [-5.3, 3.8]\,. \tag{6.8}$$

This bound improves on the LHC Run I constraint (6.4) by a factor of around 2.5. Notice that in this case the non-SM solution present in (5.3) would be fully removed by the combination of $gg \to h$ and $h \to \gamma\gamma$.

7 Conclusions

In this article, we have proposed to constrain deviations in the trilinear Higgs coupling λ by studying Higgs production in gluon-gluon-fusion and diphoton Higgs decays. To keep our discussion general, we have employed the SM EFT, in which new-physics effects are described by dimension-6 operators. In this framework, we have calculate 2-loop contributions to the $gg \to h$ and $h \to \gamma\gamma$ amplitudes that are affected by insertions of the effective operator $O_6 = -\lambda \left(H^\dagger H\right)^3$. By an explicit calculation of the complete 2-loop anomalous dimensions involving a single insertion of O_6, we have shown that the effective hgg and $h\gamma\gamma$ couplings do not receive logarithmically-enhanced contributions proportional to $\bar{c}_6$. The leading contributions to the $gg \to h$ and $h \to \gamma\gamma$ transitions involving the Wilson coefficient of O_6 are hence finite and arise from 2-loop Green's functions with modified interaction vertices. We have calculated these corrections by employing a heavy-mass expansion procedure.

Assuming that $\bar{c}_6$ is the only Wilson coefficient that receives a non-vanishing correction at the scale where new physics enters, we have analysed the sensitivity of present and future measurements of the signal strengths in $gg \to h$ and $h \to \gamma\gamma$. In particular, we have demonstrated that the indirect constraints on $\bar{c}_6$ that follow from a combination of the LHC Run I measurements of Higgs production in gluon-gluon-fusion and diphoton Higgs decays are more stringent than a direct extraction that uses the recent ATLAS upper limit on double-Higgs production. Our novel 95% CL bound of $\bar{c}_6 \in [-12.7, 9.9]$ implies that the trilinear Higgs coupling can at the moment still deviate from its SM value by a factor of approximately 11.

We have furthermore investigated the prospects of the indirect constraints at future high-energy colliders. In the case of the HL-LHC with $3\,\text{ab}^{-1}$ of integrated luminosity, we have found that it should be possible to improve the present bound by a factor of more than 1.5, while for a FCC-ee an improvement by a factor of 2.5 seems feasible. The indirect tests proposed in our work could thus become sensitive to $|\bar{c}_6| \simeq 5$, while studies of double-Higgs production at the LHC may ultimately allow to set a 95% CL bound of $\bar{c}_6 \in [-2.3, 7.7]$. The sensitivity of our proposal is hence not sufficient to compete with the constraints of $pp \to 2h$ for what concerns the solution close to $\bar{c}_6 = 0$, but it should allow to remove parts of the flipped-sign solution centred around $\bar{c}_6 \simeq 5.7$.

While the proposed indirect probes of λ can clearly not replace the direct extraction of the trilinear Higgs coupling at the LHC through double-Higgs production, we believe that they may turn out to be very valuable when included into a global analysis of Wilson coefficients, because compared to the direct measurement they constrain different linear combinations of effective operators in the SM EFT. An extension of our analysis of indirect probes to other Higgs measurements, electroweak precision observables or quark flavour physics thus seems worthwhile and will be considered elsewhere.

Acknowledgments

We thank Florian Goertz for valuable discussions concerning double-Higgs production at the HL-LHC. The work of MG has been supported by the STFC consolidated grant

ST/L000431/1. UH acknowledges the hospitality and support of the CERN theory division. He also would like to thank the KITP in Santa Barbara for hospitality and acknowledges that this research was supported in part by the National Science Foundation under Grant No. NSF PHY11-25915. UH is finally grateful to the MITP in Mainz for its hospitality and its partial support during the completion of this work.

A Non-physical operators

In addition to the gauge-invariant operators (2.2), non-physical operators arise as counterterms in the renormalisation of higher loop one-particle-irreducible off-shell Green's functions with an insertion of the operator O_6. These non-physical operators can in general be divided into operators that vanish by the use of the equations of motion (EOM), non-physical counterterms that can be written as a Becchi-Rouet-Stora-Tyutin (BRST) variation of other operators, i.e. so-called BRST-exact operators, and evanescent operators that vanish algebraically in $d = 4$ dimensions.

For the calculation of the 2-loop anomalous dimensions that describes the mixing of O_6 into O_k, it turns out that BRST-exact and evanescent operators do not play a role, and that only a single EOM-vanishing operator is necessary. This operator can be written as

$$\begin{aligned} N_1 = H^\dagger H \Big[& H^\dagger \big[D_\mu D^\mu H\big] + \big[D_\mu \left(D^\mu H\right)^\dagger\big] H \\ & - m_h^2 \left(1 - \frac{3\bar{c}_6}{4}\right) H^\dagger H + 4\lambda \left(1 - \frac{3\bar{c}_6}{2}\right) \left(H^\dagger H\right)^2 \\ & + \Big(Y_u\, \bar{Q}_L u_R \tilde{H} + Y_d\, \bar{Q}_L d_R H + Y_\ell\, \bar{L}_L \ell_R H + \text{h.c.}\Big) \Big] . \end{aligned} \tag{A.1}$$

The terms $\bar{c}_6$ appear here because λ denotes the combination $m_h^2/(2v^2)$ of the Higgs mass m_h and its VEV v $\big($see (1.2)$\big)$ and not the coefficient multiplying the quartic coupling $(H^\dagger H)^2$ entering the SM Higgs potential. At the order we are working the terms proportional to $\bar{c}_6$ do not contribute to (3.2). Note that the EOM-vanishing operator N_1 arises as a counterterm independently of the IR regularisation adopted in the computation of the 2-loop anomalous dimensions of O_6. However, if the regularisation respects the underlying symmetry, and all the diagrams are calculated on-shell, non-physical operators have vanishing matrix elements. In this case the operator given in (A.1) would not contribute to the mixing of physical operators. If the gauge symmetry is broken this is no longer the case, as graphs with insertions of non-physical operators will generally project onto physical operators. Since our IR regularisation implies massive boson propagators, non-physical counterterms play a crucial role at intermediate stages of our anomalous dimensions calculation.

B Feynman rules

Inserting the explicit form of the SM Higgs doublet

$$H = \begin{pmatrix} \phi^+ \\ \frac{1}{\sqrt{2}} \left(v + h + i\phi^0\right) \end{pmatrix} , \tag{B.1}$$

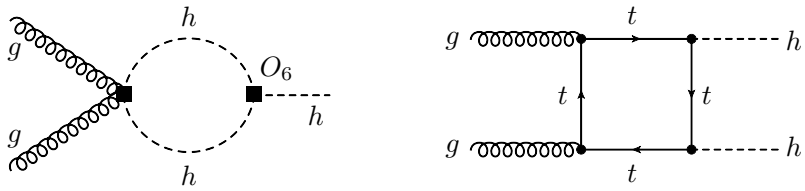

Figure 3. Left: UV divergent 1-loop diagram that involves the insertion of an effective $gghh$ and h^3 vertex. Right: An example of a 1-loop diagram that gives rise to an effective $gghh$ interaction after the top quark has been integrated out.

into the expression for O_6 as given in (2.2), one obtains the following interactions

$$\begin{aligned} O_6 \supset -\Big[& vh^3 + \frac{3}{2}h^4 + \frac{3}{2}h^2\left((\phi^0)^2 + 2\phi^+\phi^-\right) + \frac{3}{4v}h^5 \\ & + \frac{3}{2v}h^3\left((\phi^0)^2 + 2\phi^+\phi^-\right) + \frac{3}{4v}h\left((\phi^0)^2 + 2\phi^+\phi^-\right)^2\Big]\lambda v^2 \,. \end{aligned} \tag{B.2}$$

Notice that O_6 does not contain a 3-point interaction of the form $h\phi^+\phi^-$, but 4-point interactions like $h^2\phi^+\phi^-$ and $h^2(\phi^0)^2$ as well as 5-point interactions such as $h^3\phi^+\phi^-$ and $h\,(\phi^0)^2\,\phi^+\phi^-$.

C Renormalisation procedure for $gg \to h$ and $h \to \gamma\gamma$

In this appendix we briefly describe the renormalisation procedure that leads to our results (4.6) and (4.10). We start with the $\mathcal{O}(\lambda)$ corrections to the $gg \to h$ amplitude. In the limit of infinitely heavy top quark, we find the following unrenormalised 2-loop amplitude

$$\mathcal{A}^{(1)}_{\rm un}(gg \to h) = \frac{\alpha_s}{\pi v}\frac{\lambda \bar{c}_6}{(4\pi)^2}\left[-\frac{1}{4\epsilon} - \frac{1}{2}\ln\frac{\mu_w^2}{m_t^2} - \frac{25}{48}\right] , \tag{C.1}$$

where $\epsilon = (4-d)/2$. The renormalised 2-loop amplitude is obtained by adding to (C.1) the counterterm contribution

$$\mathcal{A}^{(1)}_{\rm ct}(gg \to h) = \frac{\lambda \bar{c}_6}{(4\pi)^2}\frac{12v}{\epsilon}\left\{\frac{\alpha_s}{48\pi v^2}\left[1 + \epsilon\left(\ln\frac{\mu_w^2}{m_t^2} + 2\right)\right]\right\} . \tag{C.2}$$

Here the first term proportional to $\bar{c}_6$ arises from the fact that for $\tau_t \to \infty$ the operator O_6 leads to a UV divergent ggh matrix element through a 1-loop diagram involving an effective $gghh$ coupling. The term in the curly brackets, on the other hand, represents the result for the 1-loop amplitude of $gg \to hh$ in the infinite top-quark mass limit, including terms up to $\mathcal{O}(\epsilon)$. The corresponding Feynman graphs are depicted in Figure 3. Notice that subtracting the counterterm contribution (C.2) from the unrenormalised result (C.1), leads to the finite correction (4.6) that is independent of IR physics, i.e. our result for $c_g^{(1)}$ does not depend on how light degrees of freedom are treated in the calculation.

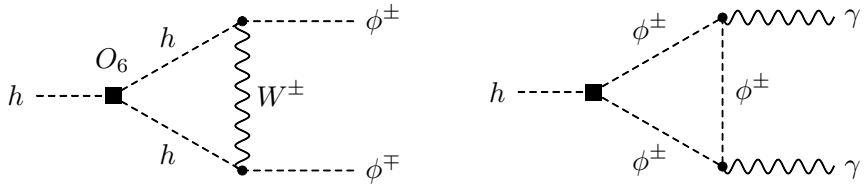

Figure 4. Left: Diagram with an insertion of O_6 that leads to a UV divergent contribution to the $h\phi^+\phi^-$ amplitude at the 1-loop level. Right: Feynman diagram that is needed to cancel the UV poles of the 2-loop $h \to \gamma\gamma$ diagrams involving a divergent $h\phi^+\phi^-$ subgraph. The black box indicates a counterterm insertion here.

In the case of $h \to \gamma\gamma$, we instead find the following unrenormalised 2-loop amplitude

$$\mathcal{A}^{(1)}_{\text{un}}(h \to \gamma\gamma) = \frac{\alpha}{\pi v} \frac{\lambda \bar{c}_6}{(4\pi)^2} \left[\frac{11}{4\epsilon} + \frac{11}{2} \ln \frac{\mu_w^2}{m_W^2} + \frac{35}{8} \right] , \tag{C.3}$$

in the limit $\tau_W \to \infty$. The corresponding counterterm takes the form

$$\begin{aligned} \mathcal{A}^{(1)}_{\text{ct}}(h \to \gamma\gamma) = & \frac{\lambda \bar{c}_6}{(4\pi)^2} \frac{12v}{\epsilon} \left\{ -\frac{7\alpha}{32\pi v^2} \left[1 + \epsilon \left(\ln \frac{\mu_w^2}{m_W^2} + \frac{44}{21} \right) \right] \right\} \\ & + \frac{\alpha}{\pi} \frac{\lambda \bar{c}_6}{(4\pi)^2} \frac{3v}{2\epsilon s_w^2} \left\{ -\frac{s_w^2}{12v^2} \left(1 + \epsilon \ln \frac{\mu_w^2}{m_W^2} \right) \right\} , \end{aligned} \tag{C.4}$$

where s_w denotes the sine of the weak mixing angle. The counterterm contribution has been split into two parts. The first one represents (in full analogy to the case of $gg \to h$) the product of the UV divergent 1-loop matrix element involving O_6 and an effective $hh\gamma\gamma$ vertex times the gauge-boson contribution to the 1-loop $hh \to \gamma\gamma$ amplitude, evaluated for $m_W \gg m_h$. The second term subtracts the UV divergences of the 2-loop diagrams that contain a divergent $h\phi^+\phi^-$ subgraph. The relevant 1-loop diagrams needed for this subtraction are shown Figure 4. The graph on the left-hand side leads to the UV pole in the second line of (C.4), while the right diagram gives rise to the expression inside the curly bracket.

D Unphysical Higgs sector

To first order in λ the charged would-be Goldstone boson propagator receives corrections from the Feynman diagrams shown in Figure 5, and similar graphs involving a virtual exchange of a neutral would-be Goldstone boson ϕ^0. The calculation of the renormalised 1-loop Goldstone selfenergies requires a renormalisation condition that involves tadpoles. The most common ways to fix the tadpole contributions consists in requiring that the effective potential contains no term linear in the Higgs field [54] or in employing the $\overline{\text{MS}}$ scheme [55, 56]. After a simple calculation it turns out that the $\mathcal{O}(\lambda)$ corrections to the Goldstone selfenergies cancel irrespectively of the precise treatment of the tadpoles. This is a result of gauge invariance.

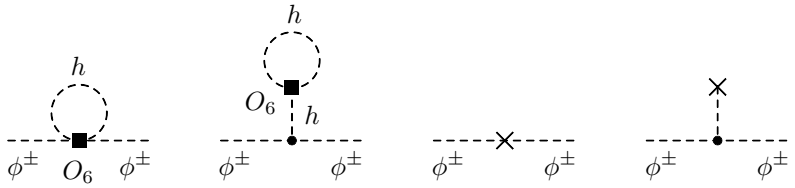

Figure 5. Feynman graphs with an insertion of O_6 (black box) that contribute to the selfenergy of the charged would-be Goldstone bosons $\phi^\pm$ at the 1-loop level. The corresponding counterterm (black cross) diagrams are also shown.

The vanishing of the $\mathcal{O}(\lambda)$ corrections to the $\phi^\pm$ selfenergies implies that in the calculation of the coefficient $c_\gamma^{(1)}$ $\big($see (4.7)$\big)$ one does not have to consider 2-loop diagrams that involve a 1-loop correction to charged would-be Goldstone boson propagators. One can furthermore show that 2-loop $\mathcal{O}(\lambda)$ contributions that arise from the $h^3\phi^+\phi^-$ or $h\,(\phi^0)^2\,\phi^+\phi^-$ parts of O_6 $\big($see (B.2)$\big)$ are cancelled by 1-loop counterterm contributions, and that this cancellation is again independent of the precise treatment of the unphysical Higgs sector, as long as the procedure respects gauge invariance.

References

[1] G. Aad *et al.* [ATLAS Collaboration], Eur. Phys. J. C **76**, no. 1, 6 (2016) [arXiv:1507.04548 [hep-ex]].

[2] V. Khachatryan *et al.* [CMS Collaboration], Eur. Phys. J. C **75**, no. 5, 212 (2015) [arXiv:1412.8662 [hep-ex]].

[3] T. Plehn and M. Rauch, Phys. Rev. D **72**, 053008 (2005) [hep-ph/0507321].

[4] T. Binoth, S. Karg, N. Kauer and R. Rückl, Phys. Rev. D **74**, 113008 (2006) [hep-ph/0608057].

[5] F. Maltoni, E. Vryonidou and M. Zaro, JHEP **1411**, 079 (2014) [arXiv:1408.6542 [hep-ph]].

[6] E. W. N. Glover and J. J. van der Bij, Nucl. Phys. B **309**, 282 (1988).

[7] T. Plehn, M. Spira and P. M. Zerwas, Nucl. Phys. B **479**, 46 (1996) [Erratum-ibid. B **531**, 655 (1998)] [hep-ph/9603205].

[8] S. Dawson, S. Dittmaier and M. Spira, Phys. Rev. D **58**, 115012 (1998) [hep-ph/9805244].

[9] A. Djouadi, W. Kilian, M. Mühlleitner and P. M. Zerwas, Eur. Phys. J. C **10**, 45 (1999) [hep-ph/9904287].

[10] D. de Florian and J. Mazzitelli, Phys. Rev. Lett. **111**, 201801 (2013) [arXiv:1309.6594 [hep-ph]].

[11] J. Grigo, J. Hoff, K. Melnikov and M. Steinhauser, Nucl. Phys. B **875**, 1 (2013) [arXiv:1305.7340 [hep-ph]].

[12] S. Borowka, N. Greiner, G. Heinrich, S. P. Jones, M. Kerner, J. Schlenk, U. Schubert and T. Zirke, Phys. Rev. Lett. **117**, no. 1, 012001 (2016) [Erratum-ibid. **117**, no. 7, 079901 (2016)] [arXiv:1604.06447 [hep-ph]].

[13] U. Baur, T. Plehn and D. L. Rainwater, Phys. Rev. D **67**, 033003 (2003) [hep-ph/0211224].

[14] U. Baur, T. Plehn and D. L. Rainwater, Phys. Rev. D **69**, 053004 (2004) [hep-ph/0310056].

[15] M. J. Dolan, C. Englert and M. Spannowsky, JHEP **1210**, 112 (2012) [arXiv:1206.5001 [hep-ph]].

[16] J. Baglio, A. Djouadi, R. Gröber, M. M. Mühlleitner, J. Quevillon and M. Spira, JHEP **1304**, 151 (2013) [arXiv:1212.5581 [hep-ph]].

[17] A. J. Barr, M. J. Dolan, C. Englert and M. Spannowsky, Phys. Lett. B **728**, 308 (2014) [arXiv:1309.6318 [hep-ph]].

[18] M. J. Dolan, C. Englert, N. Greiner and M. Spannowsky, Phys. Rev. Lett. **112**, 101802 (2014) [arXiv:1310.1084 [hep-ph]].

[19] A. Papaefstathiou, L. L. Yang and J. Zurita, Phys. Rev. D **87**, no. 1, 011301 (2013) [arXiv:1209.1489 [hep-ph]].

[20] F. Goertz, A. Papaefstathiou, L. L. Yang and J. Zurita, JHEP **1306**, 016 (2013) [arXiv:1301.3492 [hep-ph]].

[21] P. Maierhöfer and A. Papaefstathiou, JHEP **1403**, 126 (2014) [arXiv:1401.0007 [hep-ph]].

[22] D. E. Ferreira de Lima, A. Papaefstathiou and M. Spannowsky, JHEP **1408**, 030 (2014) [arXiv:1404.7139 [hep-ph]].

[23] C. Englert, F. Krauss, M. Spannowsky and J. Thompson, Phys. Lett. B **743**, 93 (2015) [arXiv:1409.8074 [hep-ph]].

[24] T. Liu and H. Zhang, arXiv:1410.1855 [hep-ph].

[25] F. Goertz, A. Papaefstathiou, L. L. Yang and J. Zurita, JHEP **1504**, 167 (2015) [arXiv:1410.3471 [hep-ph]].

[26] ATLAS Collaboration, http://cds.cern.ch/record/1956733/files/ATL-PHYS-PUB-2014-019.pdf

[27] A. Azatov, R. Contino, G. Panico and M. Son, Phys. Rev. D **92**, no. 3, 035001 (2015) [arXiv:1502.00539 [hep-ph]].

[28] A. Carvalho, M. Dall'Osso, T. Dorigo, F. Goertz, C. A. Gottardo and M. Tosi, JHEP **1604**, 126 (2016) [arXiv:1507.02245 [hep-ph]].

[29] ATLAS Collaboration, http://cds.cern.ch/record/2065974/files/ATL-PHYS-PUB-2015-046.pdf

[30] M. McCullough, Phys. Rev. D **90**, no. 1, 015001 (2014) Erratum: [Phys. Rev. D **92**, no. 3, 039903 (2015)] [arXiv:1312.3322 [hep-ph]].

[31] C. Shen and S. h. Zhu, Phys. Rev. D **92**, no. 9, 094001 (2015) [arXiv:1504.05626 [hep-ph]].

[32] J. Elias-Miró, J. R. Espinosa, E. Masso and A. Pomarol, JHEP **1308**, 033 (2013) [arXiv:1302.5661 [hep-ph]].

[33] E. E. Jenkins, A. V. Manohar and M. Trott, JHEP **1310**, 087 (2013) [arXiv:1308.2627 [hep-ph]].

[34] E. E. Jenkins, A. V. Manohar and M. Trott, JHEP **1401**, 035 (2014) [arXiv:1310.4838 [hep-ph]].

[35] R. Alonso, E. E. Jenkins, A. V. Manohar and M. Trott, JHEP **1404**, 159 (2014) [arXiv:1312.2014 [hep-ph]].

[36] K. G. Chetyrkin, M. Misiak and M. Münz, Nucl. Phys. B **518**, 473 (1998) [hep-ph/9711266].

[37] P. Gambino, M. Gorbahn and U. Haisch, Nucl. Phys. B **673**, 238 (2003) [hep-ph/0306079].

[38] M. Gorbahn and U. Haisch, Nucl. Phys. B **713**, 291 (2005) [hep-ph/0411071].

[39] L. Avdeev, J. Fleischer, S. Mikhailov and O. Tarasov, Phys. Lett. B **336**, 560 (1994) [Phys. Lett. B **349**, 597 (1995)] [hep-ph/9406363].

[40] W. Buchmüller and D. Wyler, Nucl. Phys. B **268**, 621 (1986).

[41] B. Grzadkowski, M. Iskrzynski, M. Misiak and J. Rosiek, JHEP **1010**, 085 (2010) [arXiv:1008.4884 [hep-ph]].

[42] M. A. Shifman, A. I. Vainshtein and V. I. Zakharov, Phys. Lett. B **78**, 443 (1978).

[43] C. Anastasiou, R. Boughezal and F. Petriello, JHEP **0904**, 003 (2009) [arXiv:0811.3458 [hep-ph]].

[44] A. Denner, G. Weiglein and S. Dittmaier, Nucl. Phys. B **440**, 95 (1995) [hep-ph/9410338].

[45] G. Aad *et al.* [ATLAS Collaboration], Phys. Rev. Lett. **114**, no. 8, 081802 (2015) [arXiv:1406.5053 [hep-ex]].

[46] G. Aad *et al.* [ATLAS Collaboration], Eur. Phys. J. C **75**, no. 9, 412 (2015) [arXiv:1506.00285 [hep-ex]].

[47] G. Aad *et al.* [ATLAS Collaboration], Phys. Rev. D **92**, 092004 (2015) [arXiv:1509.04670 [hep-ex]].

[48] J. Alwall *et al.*, JHEP **1407**, 079 (2014) [arXiv:1405.0301 [hep-ph]].

[49] V. Hirschi and O. Mattelaer, JHEP **1510**, 146 (2015) [arXiv:1507.00020 [hep-ph]].

[50] R. Gröber, M. Mühlleitner, M. Spira and J. Streicher, JHEP **1509**, 092 (2015) [arXiv:1504.06577 [hep-ph]].

[51] See M. Spira's webpage http://tiger.web.psi.ch/hpair/

[52] CMS Collaboration, https://cds.cern.ch/record/1494600/files/NOTE2012_006.pdf

[53] M. Ruan, arXiv:1411.5606 [hep-ex].

[54] A. Denner, Fortsch. Phys. **41**, 307 (1993) [arXiv:0709.1075 [hep-ph]].

[55] F. Jegerlehner, M. Y. Kalmykov and O. Veretin, Nucl. Phys. B **641**, 285 (2002) [hep-ph/0105304].

[56] F. Jegerlehner, M. Y. Kalmykov and O. Veretin, Nucl. Phys. B **658**, 49 (2003) [hep-ph/0212319].